

IMAGES OF FOUR COMPACT STEEP-SPECTRUM QUASARS WITH A RESOLUTION OF
20 MILLIARCSECONDS AT 329.1 MHzR. S. SIMON,¹ A. C. S. READHEAD, AND A. T. MOFFET²
Owens Valley Radio Observatory, California Institute of Technology
P. N. WILKINSON AND R. BOOTH³
Nuffield Radio Astronomy Laboratories

AND

B. ALLEN⁴ AND B. F. BURKE
Massachusetts Institute of Technology
Received 1989 June 27; accepted 1989 November 6

ABSTRACT

Four compact steep-spectrum quasars (3C 48, 3C 147, 3C 309.1, and 3C 380) have been mapped with a resolution of 20 mas at 329 MHz. The structures of all four objects are asymmetric and complex, but they are shown here to be consistent with a basic one-sided jet morphology. In this, they are quite similar to other classes of radio sources; however, their small scales and convoluted structures suggest that in these objects, other factors such as the interaction with the interstellar medium and/or variations in the initial jet direction significantly affect the morphology.

Subject headings: galaxies: jets — interferometry — quasars

I. INTRODUCTION

Compact steep-spectrum radio sources (hereafter CSS sources) (Kapahi 1981; Peacock and Wall 1982) have no obvious relation to the other classes of radio sources (e.g., Pearson and Readhead 1988). The structures, on kiloparsec scales, of the quasars in this class are much more complex than those of either classical double sources or compact, flat-spectrum objects (Wilkinson *et al.* 1984c; Fanti *et al.* 1984, 1985, 1986, 1988). Many CSS objects exhibit turnovers in their overall radio spectra in the range 0.1 to 1 GHz which are generally ascribed to synchrotron self-absorption (e.g., Jones, O'Dell, and Stein 1974; Scott and Readhead 1977). The angular sizes of the major emission regions in many of these objects have been shown by interplanetary scintillation observations to be less than 1" (Readhead and Hewish 1974), which is significantly smaller than the width of the outer lobes in most double-lobed radio sources. Thus, most of these objects are intrinsically small and not just normal double-lobed quasars viewed end-on.

In this paper, we present maps of four CSS objects (3C 48, 3C 147, 3C 309.1, and 3C 380) at 329.1 MHz with 20 mas resolution, and we compare these with both VLBI and VLA maps at other frequencies. We show that the nuclear structures observed in all these objects are one-sided jets which bend through projected angles greater than 90° and are very asymmetric. Three of these objects (3C 147, 3C 309.1, and 3C 380) have some large-scale radio emission on the side opposite the jet. Thus, they could well be two-sided jets in which the jet directed away from the line of sight is rendered invisible by anisotropic emission. The fourth object (3C 48) shows no evidence of radio emission on the side opposite the jet and is the most unusual of the four objects. Some of these objects have

highly convoluted structures. The bends are ascribed to interaction between the jet and surrounding interstellar medium and/or variations in the initial jet direction. If the bends are caused by interaction with the surrounding medium, this interaction must be significantly greater in these objects than in the double-lobed and compact flat-spectrum objects and may be indicative of recent mergers in this class of object.

II. THE OBSERVATIONS

The observations were made during a 54 hr VLBI experiment from 1800 UT on 1981 January 30 to 2400 UT on 1981 February 1. A seven station network (see Table 1) was used at a center frequency of 329.1 MHz. In order to maximize the u , v coverage, each object was observed for about 12 hr. Table 2 lists the number of baseline hours observed on each source. There were no major problems at any station lasting more than a few hours, and extensive observations were obtained of each object.

The observations were recorded at each telescope in standard Mk II format (Clark 1973), with an effective recording bandwidth of 1.8 MHz. The tapes were processed in three passes on the five station Caltech/JPL VLBI correlator in Pasadena.

After correlation, it was necessary to edit the data to remove spurious and degraded data points. There were several causes of degradation. Severe problems were encountered due to loss of coherence. The maximum usable coherent integration time for each source was set by the time scale for phase variations due to electron density fluctuations in both the interplanetary medium and the ionosphere. Because these observations were made near the solar maximum in 1981, the ionosphere was in a highly disturbed state, and coherence times were typically on the order of 30–60 s. This contrasts with observations made at this frequency in 1975 (Simon *et al.* 1980), for which the coherence time was on the order of 4 minutes. In addition, the coherence time was not constant throughout the observations, but it varied strongly with position on the sky and weakly with

¹ Now at the E. O. Hulburt Center for Space Research.

² Deceased.

³ Now at the Chalmers Technical University.

⁴ Now at TRW.

TABLE 1
INTERFEROMETER ELEMENTS

Station Name	Location	Diameter (m)	System Temperature (K)	Sensitivity (K Jy ⁻¹)
JBNK	Jodrell Bank, Cheshire	76	270	0.63
HSTK	Haystack, MA	46	220 ^a	0.21
NRAO	Greenbank, WV	43	125	0.21
IOWA	North Liberty, IA	18	160	0.042
FDVS	Fort Davis, TX	26	340	0.06
OVRO	Big Pine, CA	40	195	0.18
HCRK	Hat Creek, CA	26	210	0.06

^a System temperatures at Haystack were about 360 K for the observations on 3C 48 and 3C 309.1.

time of day. In the case of 3C 309.1, for example, the coherence time varied from less than 15 s at the start to longer than 30 s on all baselines at the end (and was then 60 s on a few baselines). For the other sources, coherence times also varied by up to a factor of 2. Coherence times were slightly longer when both stations on a baseline were in darkness. Observations with the MERLIN array (Davies, Anderson, and Morrison, 1980) on baselines of 6 to 135 km have also shown this effect.

The coherence time was also weakly anticorrelated with baseline length up to about 1000 km. This is significantly longer than the typical scale sizes observed in the ionosphere (e.g., Hewish 1952), which is 2 to 10 km, and it is comparable to the scale sizes observed in the interplanetary medium (Readhead, Kemp, and Hewish 1978). It is likely that the interplanetary medium had a significant effect on the coherence times on all the sources. More recent 329 MHz VLBI observations (Simon *et al.* 1988) clearly demonstrate that for sources within $\sim 80^\circ$ of the Sun, the interplanetary medium causes 1 rad and larger phase fluctuations on time scales of ~ 30 s.

For the purposes of this work, the causes of the short coherence times are unimportant; their effect was to force us to adjust the coherent integration times throughout the correlation of the data. To minimize the effects of coherence losses, we used relatively short integration times (see Table 2). With the coherent integration time chosen near the maximum permissible, occasional data points were significantly reduced in fringe amplitude. This leads to nonclosing amplitude errors and higher phase noise. We therefore discarded data points which were affected by loss of coherence. Up to a few percent of the observations on each object were deleted for this reason. This analysis was performed before the availability of global fringe fitting algorithms (e.g., see Schwab and Cotton 1983); such algorithms would have resulted in an improvement in the data quality.

TABLE 2
SOURCES OBSERVED

Name	IAU Designation	z	329 MHz Flux Density	Baseline Hours	Typical Coherence Time (s)
3C 48	0134+32	0.3670	43.5	115	60
3C 147	0538+49	0.545	53	204	60
3C 309.1	1458+71	0.904	16	215	30
3C 380	1828+48	0.691	42	174	60-120

We were also troubled by radio frequency interference. A burst of interference affects the observations at a particular station for a brief period. The resulting increase in system temperature causes a reduction in fringe amplitude. We therefore deleted anomalously low fringe amplitudes and their associated phases. After editing, the data were incoherently averaged for 3 minutes (3C 380) or 4 minutes (3C 48, 3C 147, and 3C 309.1) and were then calibrated using the procedure of Cohen (1973).

Due to inconsistencies in the measured antenna temperatures at different stations and varying system temperature measurements, it was not possible to make a final calibration for the entire experiment from the calibration data for each station alone. As a result, the final calibration for each antenna was not determined until the maps were made. In addition to the above problems, there are several other effects which can lead to baseline-related offsets in both amplitude and phase. These have recently been discussed by Cornwell (1986) and by Wilkinson, Conway, and Biretta (1988). For these observations, we believe that poorly matched passband defining filters are likely to be the dominant source of such errors (up to 10%). Other errors can arise from:

- i) Nonidentical antenna polarizations.
- ii) Imperfect coherence; also, at low frequencies differential Faraday rotation through the ionosphere can also cause additional decorrelation if the telescope feeds are sensitive to a component of linear polarization (see, e.g., Slee and Wraith 1967) — this effect is in addition to the polarization effect mentioned by Wilkinson, Conway, and Biretta (1988).
- iii) Tape playback errors.
- iv) Positive bias resulting from incoherent averaging of the data on insensitive baselines (see, e.g., Moran 1976).

The final maps produced from these data have a dynamic range (i.e., the ratio of the peak flux density on the map to the rms flux density in a blank region of sky) which is limited by these errors to about 200:1.

We have assumed a Hubble constant of $H_0 = 100h$ km s⁻¹ Mpc⁻¹ and $q_0 = 0.5$ in order to convert angular measurements into physical scales and distances.

III. THE MAPS

Originally, maps of these sources were made with the Caltech version of the Cornwell and Wilkinson (1981) self-calibration procedure (Simon 1983; Wilkinson *et al.* 1984a). However, it was clear that the off-source noise level in these maps was too high, indicating that systematic errors in the data of the types discussed above were limiting the dynamic

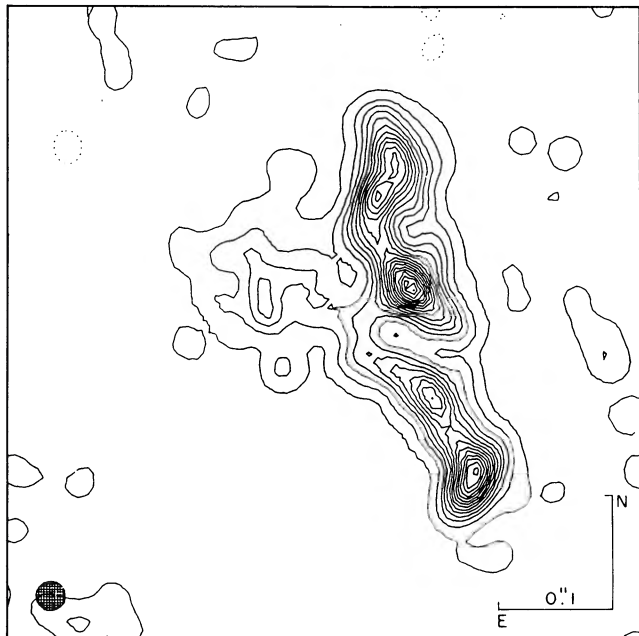


FIG. 1a

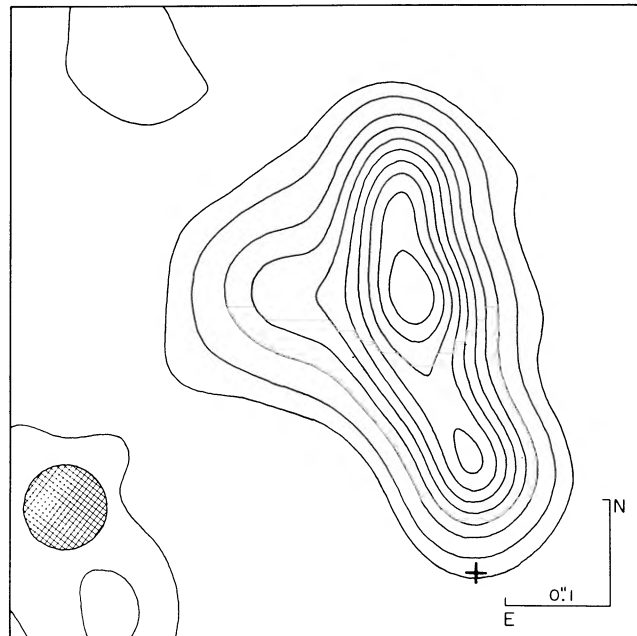


FIG. 1b

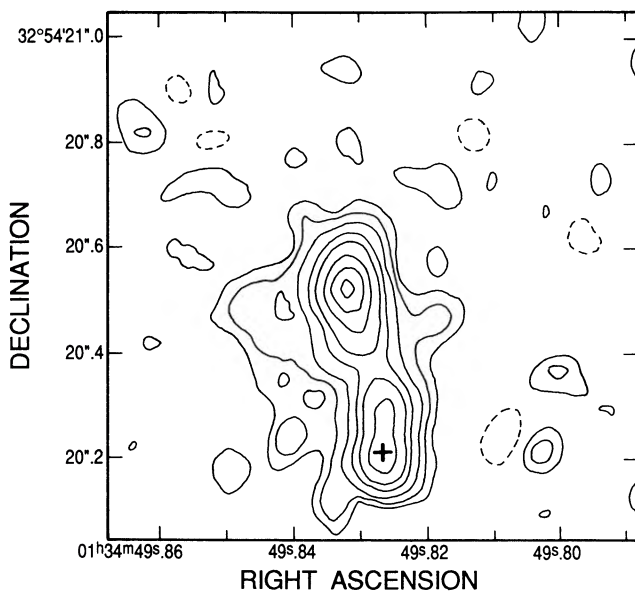


FIG. 1c

FIG. 1.—(a) 3C 48 map at 329.1 MHz with 26 mas beam. The scale is $3.1h^{-1}$ pc mas $^{-1}$. Contour levels $-3, 3, 9, 15, 21, 27, 33, 39, 45, 51, 57, 63, 69, 75, 81, 87, 93, 99\%$ of maximum ($1.26 \text{ Jy beam}^{-1}$). (b) 3C 48 map at 329.1 MHz with 80 mas beam. Contour levels $-5, 5, 10, 20, 30, 40, 50, 60, 70, 80, 90\%$ of maximum ($4.06 \text{ Jy beam}^{-1}$). (c) VLA map of 3C 48 at 22.5 GHz with 80 mas beam. The contour levels are $-2.5, 2.5, 5, 10, 20, 30, 50, 70, 90\%$ of maximum ($0.22 \text{ Jy beam}^{-1}$). This map has been reproduced prior to publication with the permission of R. Perley.

range. A critical reanalysis of the original data subsequently revealed previously unrecognized phase offsets associated with the processing and fringe-fitting step, as well as significant amplitude calibration errors. These errors were corrected and new maps were made.

The maps of 3C 147, 3C 309.1, and 3C 380 were made with the Jodrell Bank interactive software OLAF—in particular,

the “difference mapping” program “MAP,” invented and written by R. G. Noble, was used. The basic idea of “difference mapping” has been outlined by Cornwell and Wilkinson (1984), while Muxlow *et al.* (1988) have given a brief introduction to the MAP program itself. The OLAF package also allows one to remove an empirically determined amplitude and phase offset for each baseline, as described by Wilkinson, Conway, and Biretta. (1988). For our maps, the dynamic range typically improved by a factor more than 3 compared with that of the original maps. For 3C 48, however, the fidelity of the map is limited at least as much by the limited u, v coverage as by data errors, and the maps presented are those produced with the Caltech package. In general, the full resolution of our array at high declination is approximately circular, and a restoring beam of FWHM 20 mas has been used. In the case of 3C 48, which is at a lower declination, the beam is elliptical, but to make the interpretation of this complicated structure easier we have used a circular restoring beam of 26 mas corresponding to the major axis of the ellipse.

a) 3C 48

This was the most difficult of the four objects to map for two reasons. First, and most important, 3C 48 is the most complex of these sources on angular scales of 20–400 mas (50 pc–1 kpc), and it does not have a single dominant component at this frequency. The lack of a clearly identifiable “core” is also evident in EVN observations at 5 GHz made by one of us (P. N. W.). Second, 3C 48 is at lower declination (32°) than the other objects, and Haystack began observing late, so that the u, v plane coverage was significantly poorer than for the other sources. The combination of complex structure and more limited u, v coverage meant that the brightness distribution of 3C 48 was less well constrained than the other sources. There were minor, but significant, differences in the maps produced using the Caltech and the OLAF packages. The maps presented in Figures 1a and 1b were those produced with the Caltech package.

Notwithstanding our concerns over the detailed fidelity of Figure 1a, we are confident that the general shape of the source is correct, since we have unpublished maps at 609 and 1661 MHz which confirm it. There are a number of striking features seen in Figure 1a that are worthy of comment. 3C 48 has a convoluted structure which defies simple classification—in fact, it is more complicated than our map reveals, since we only account for 16 Jy of the total flux density of 43.5 Jy. The remaining 27.5 Jy must be in extended, low-brightness emission which is totally resolved by our shortest baseline. The overall extent of 3C 48 at low frequencies has been determined by the 81.5 MHz VLBI observations of Hartas *et al.* (1983); they derive a diameter of $>3'.5$.

In order to make more sense of our data, we convolved the map in Figure 1a to a resolution of 80 mas (Fig. 1b) so that we could compare it with a VLA image at 22 GHz (Fig. 1c; R. Perley, private communication). When these two images are compared, it is clear that there is a component near the southern end of the source (marked by a cross in Figs. 1b and 1c) whose spectrum rises sharply from 327 MHz to 22 GHz. We identify this as the active core of 3C 48 and can then interpret the structure as that of a one-sided jet, albeit knotty and twisted, extending from south to north.

b) 3C 147

This was the strongest of the four sources, and our map (Fig. 2a) accounts for 43 Jy of the total flux density of 53 Jy. The remaining 10 Jy is in smooth, extended structure; Hartas *et al.* (1983) show that at 81.5 MHz about 15% of the total flux density comes from emission with a characteristic size of $4''$. The inner structure of 3C 147 at 327 MHz is dominated by an unresolved core at the north eastern end of a $0'.2$ (0.75 kpc) jet. This structure is confirmed by VLBI maps made at higher frequencies (Wilkinson *et al.* 1977; Readhead and Wilkinson

1980; Simon *et al.* 1983b). The surface brightness sensitivity of our 327 MHz map is sufficient to reveal several new features of the structure. Even at this comparatively low resolution for VLBI, the jet is clearly resolved across its main axis and appears to be surrounded by a cocoon of emission; this is unusual for core-jet sources observed with VLBI. A sharp bend (through 105°) at the southwestern tip of the jet is seen more clearly in this VLBI map than in the earlier ones, and there is also low-brightness emission to the northeast and the south east of the core which was not seen in the previous VLBI maps, but these have been detected in VLA and MERLIN maps (Readhead, Napier, and Bignell 1980; van Breughel, Miley, and Heckman 1984; Wilkinson *et al.* 1984c).

We convolved our 327 MHz map down to a resolution of 50 mas (Fig. 2b) to show this emission more clearly and in order to compare it with a MERLIN map made at 5 GHz (Wilkinson *et al.* 1984c). The 327 MHz and 5 GHz maps are very similar and show that the emission in 3C 147 is, apparently, two-sided. It is possible that this is an effect of projection and the jet swings round to connect up with the northerly component; however, the present map does not show any connection between the two. Finally, it is possible that the southeastern emission seen in the 327 MHz and 5 GHz maps could be associated with other jets emanating from the core. Since this would be a feature unique to 3C 147 and would be the first evidence of poor collimation near the nucleus of a CSS source, a high-resolution, high-surface brightness sensitivity VLBI map is urgently needed to explore this possibility.

c) 3C 309.1

The map at a resolution of 20 mas is shown in Figure 3a. It reveals a one-sided jet which bends through 110° 100 mas ($400h^{-1}$ pc) from the core, which is at the northwesternmost tip (Wilkinson *et al.* 1986). The jet then apparently curves back on

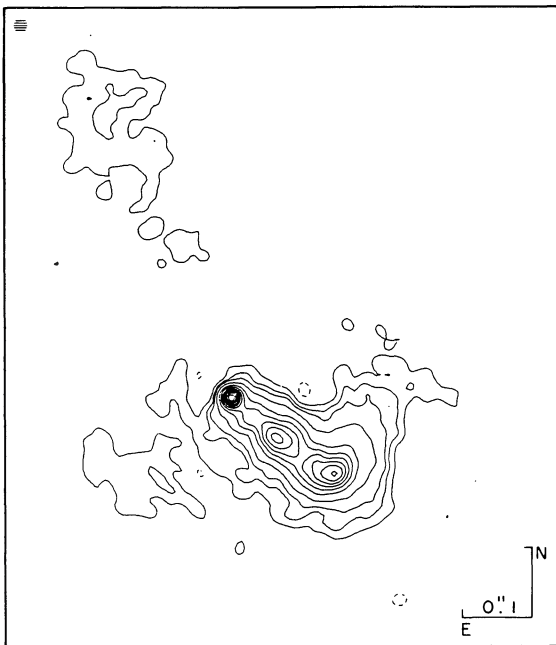


FIG. 2a

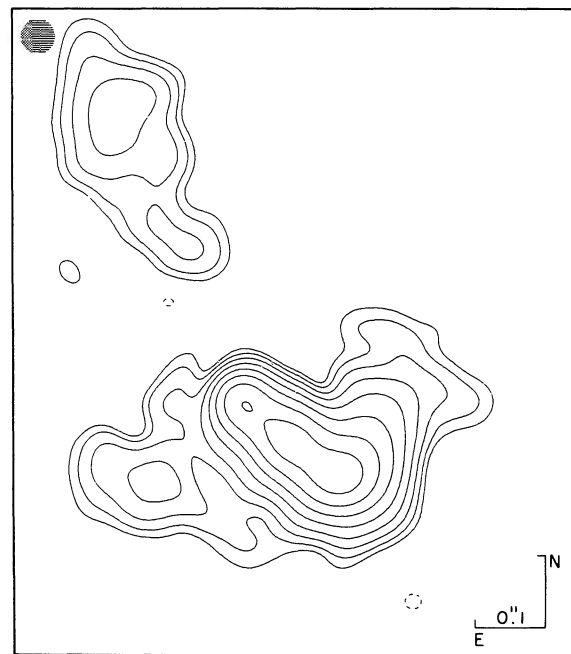


FIG. 2b

FIG. 2.—(a) 3C 147 map at 329.1 MHz with 20 mas beam. The scale is $3.7h^{-1}$ pc mas $^{-1}$. Contour levels — 1, 1, 3, 5, 10, 20, 30, 40, 50, 60, 70, 80, 90% of maximum (2.35 Jy beam $^{-1}$). (b) 3C 147 map at 329.1 MHz with 50 mas beam. Contour levels — 0.5, 0.5, 1, 2, 4, 8, 16, 32, 64% of maximum (6.37 Jy beam $^{-1}$).

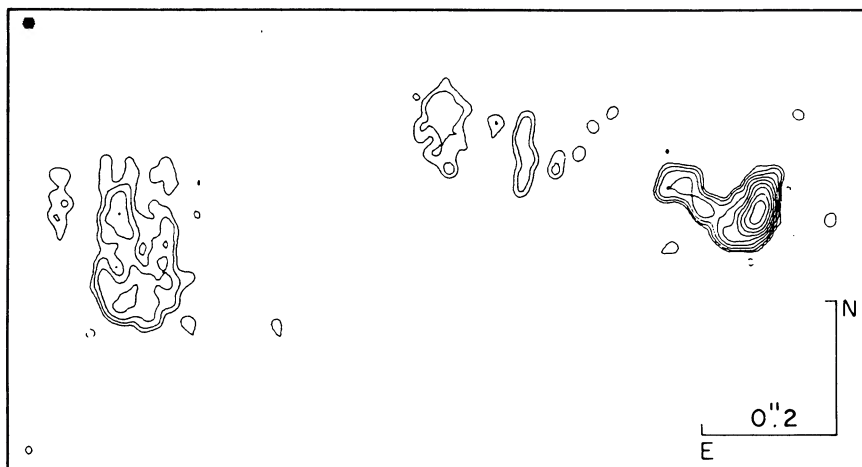


FIG. 3a

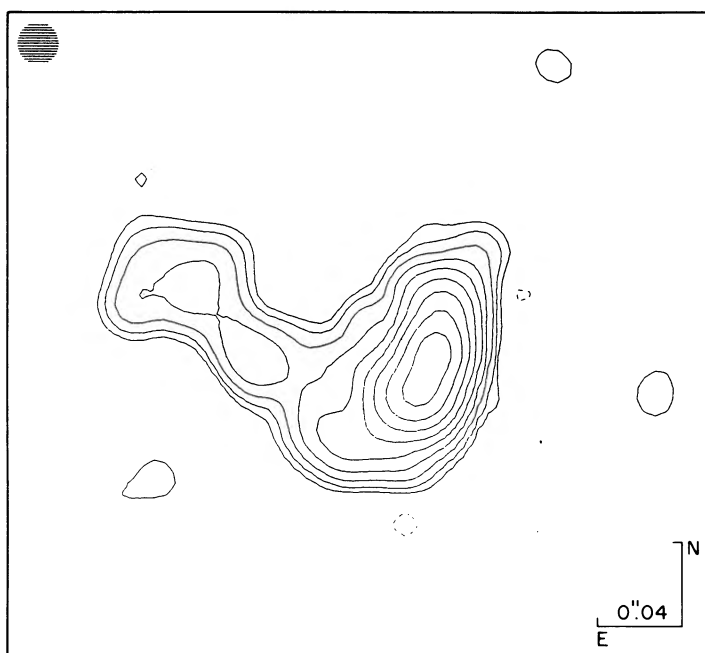


FIG. 3b

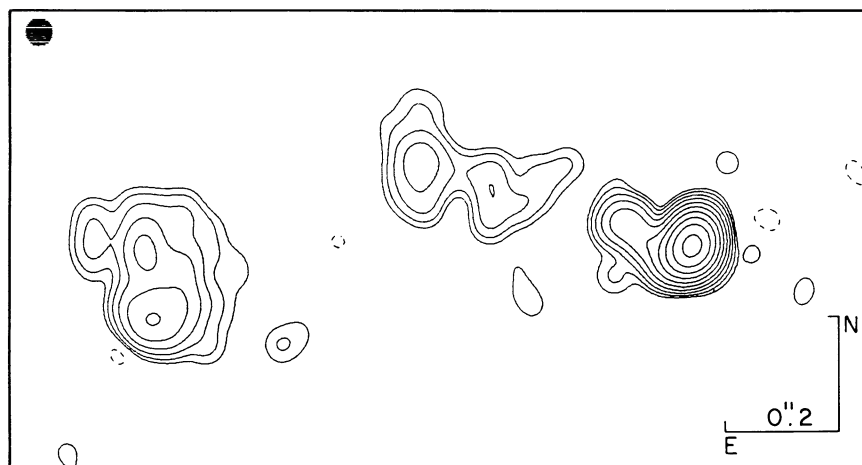


FIG. 3c

FIG. 3.—(a) 3C 309.1 map at 329.1 MHz with 20 mas beam. The scale is $4.2h^{-1}$ pc mas $^{-1}$. Contour levels $-0.3, 0.3, 0.5, 1, 2, 4, 8, 16, 32, 64\%$ of maximum (3.12 Jy beam $^{-1}$). (b) 3C 309.1 core at 329.1 MHz with 20 mas beam. Contour levels $-0.3, 0.3, 0.5, 1, 2, 4, 8, 16, 32, 64\%$ of maximum (3.12 Jy beam $^{-1}$). (c) 3C 309.1 map at 329.1 MHz with 50 mas beam. Contour levels $-0.2, 0.2, 0.3, 0.6, 1.2, 2.4, 4.8, 9.6, 19.2, 38.4, 76.8\%$ of maximum (6.04 Jy beam $^{-1}$).

itself and ends at a hot spot $1''$ ($4h^{-1}$ kpc) from the core. Our map is entirely consistent with earlier maps of the compact features in 3C 309.1 (Kus, Wilkinson, and Booth 1981; Wilkinson *et al.* 1984a, 1986) and does not reveal any weak compact components in the relaxed western lobe seen in the MERLIN map (Cornwell and Wilkinson 1981). This western lobe must contribute most of the missing flux density in our map; the total flux density of 3C 309.1 at 327 MHz is 16 Jy, and our map accounts for 11.5 Jy. The core region alone is shown in Figure 3b, and the map convolved with a 50 mas beam is shown in Figure 3c. These figures show one new aspect of the structure of 3C 309.1: during the course of its apparent bend through 110° , the jet's width and surface brightness do not change significantly. This is interesting, since the Wilkinson *et al.* (1986) 1.6 GHz VLBI map showed that the jet width increases for the first 60 mas ($240h^{-1}$ pc) of its length; our map shows that the width remains roughly constant out to about 200 mas, while the Wilkinson *et al.* (1986) MERLIN + EVN map shows that the jet then "flares" sharply just as it falls below our present detection level. The evidence is, then, that the jet is recollimated, presumably while passing through the interstellar medium (ISM) of the parent galaxy; it may be that the subsequent flaring coincides with the jet leaving the ISM, as for example has been seen in the quasar PKS 0812+020 (Ghigo *et al.* 1986). We leave a more detailed discussion of these and more recent measurements of the jet in 3C 309.1 to a later paper.

d) 3C 380

The full-resolution image of this source is presented in Figure 4a. The bright core is elongated in the direction of the "knot" located $0''.72$ ($2.9h^{-1}$ kpc) to the northwest. This knot is resolved in both dimensions and is edge-brightened on the side facing the core (see also Wilkinson *et al.* 1984a). This fact, taken with the Wilkinson *et al.* (1986) 5 GHz VLBI image of

the core region, strongly indicates that a jet emerges from a core located at the southeastern tip of the jet and extends at least as far as the $0''.72$ component. Given the convoluted appearance of 3C 380 on the arcsecond scale as mapped by MERLIN (Wilkinson *et al.* 1984a, b; Flatters 1987), this represents some progress in understanding the confusing radio structure of this source. The overall size of 3C 380 is $15''$ (Wilkinson *et al.* 1990 in preparation), and some of this extended structure is seen on our shortest baselines. In Figure 4b we show the map convolved to a resolution of 50 mas to reveal the higher brightness parts of the extended structure. The map is in good agreement with an unpublished MERLIN map at 5 GHz (C. Akujor, private communication). Further discussion of this and other recent results on 3C 380 is deferred to another paper.

IV. DISCUSSION

The four objects (3C 48, 3C 147, 3C 309.1, and 3C 380) were selected because of their strength and compact structure. Morphologically they look quite different, although they do all have one-sided core-jet morphologies, with a flat-spectrum core at one end of a steep-spectrum jet. The "cores" in these objects are strikingly different: 3C 48 has a barely visible flat spectrum core component; 3C 147 has an amorphous core which is highly resolved at higher frequencies; 3C 309.1 has a clear flat-spectrum core, which is very similar to those seen in flat-spectrum compact objects; and 3C 380 has a dominant flat-spectrum core. These morphological differences in both the cores and the jets of these objects suggest that different physical processes may dominate in different objects of the CSS class. As mentioned in the introduction, the relationship between these CSS objects and either classical double sources or compact flat-spectrum sources is unclear. There are some

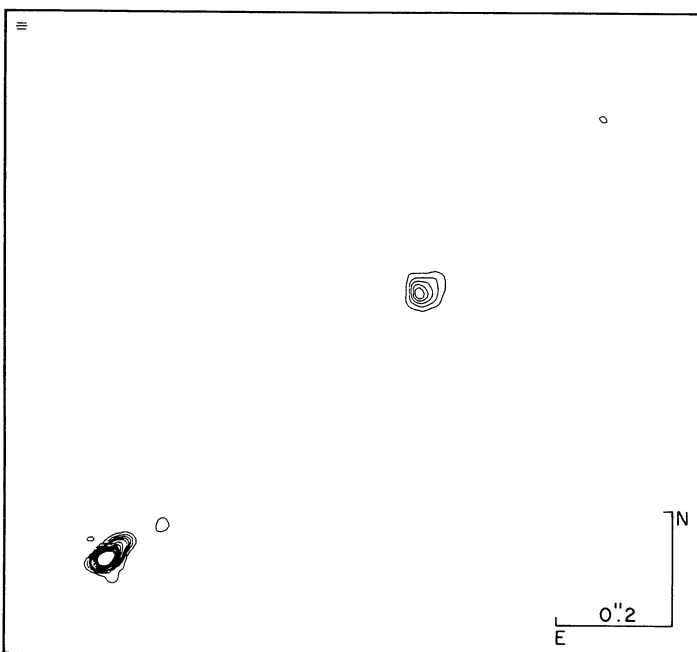


FIG. 4a

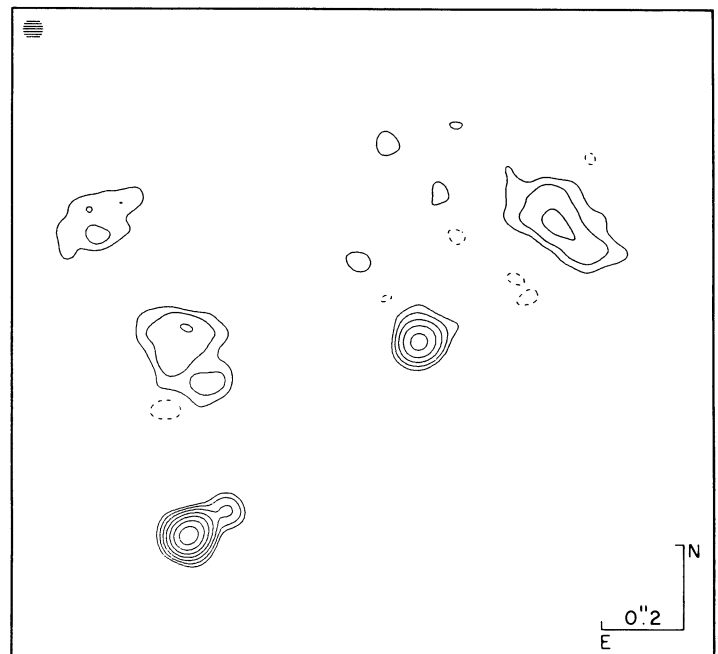


FIG. 4b

FIG. 4.—(a) 3C 380 map at 329.1 MHz with 20 mas beam. The scale is $4.0h^{-1}$ pc mas $^{-1}$. Contour levels 2, 4, 6, 8, 10, 15, 20, 25, 30, 35, 40, 45, 50% of maximum (2.00 Jy beam $^{-1}$). (b) 3C 380 map at 329.1 MHz with 50 mas beam. Contour levels $-2, -1, 1, 2, 4, 8, 16, 32, 64\%$ of maximum (3.09 Jy beam $^{-1}$).

similarities, however, between some objects of the CSS class and the other classes, namely:

1. In some of the CSS objects, there is extended structure on both sides on the core. In three of the quasars we mapped, in addition to the apparent core-jet structure, there is emission on the side of the core opposite to the main beam or jet. In 3C 147, the MERLIN map (Wilkinson *et al.* 1984c) shows weak emission roughly opposite to the jet to the northeast; a puzzling feature in that map, however, is the emission to the southeast of the core. Both these areas of emission were also detected at 329 MHz, confirming that they are real. In 3C 309.1, the emission opposite to the MERLIN arcsecond jet is in the form of a weak component about 0.9 to the west (Cornwell and Wilkinson 1981; Kus, Wilkinson, and Booth 1981; Wilkinson *et al.* 1984c). In 3C 380, it is the core which shows elongation in a direction nearly perpendicular to the position angle defined by the extended northwestern component. Finally, unpublished MERLIN observations of 3C 48 show faint, extended emission to the south on the arcsecond scale.

2. Some of the CSS objects have spectra which flatten at high frequencies. This is evidence of a flat-spectrum compact core within the CSS objects which may be similar to the flat-spectrum compact cores in the central components of classical doubles. Such sources would include 3C 48, for which we have presented evidence for a compact core with a spectrum that rises toward higher frequencies 3C 380 and 3C 216.

3. There is evidence for bulk relativistic motion in some CSS objects, such as has been seen in both of the other classes of objects. Calculations of the expected inverse Compton X-ray radiation for both 3C309.1 (Kus *et al.* 1990, in preparation) and 3C 147 (Simon *et al.* 1983a) suggest that bulk relativistic motion may be occurring in those objects. In addition, 3C 216 is a superluminal source (Barthel, Pearson, and Readhead 1988).

4. There seems to be a qualitative relationship between the

complexity of the structure in a CSS object and its optical identification. MERLIN maps (e.g., see Wilkinson *et al.* 1984a) and VLBI maps (e.g., see Fanti *et al.* 1988) show that CSS sources identified with galaxies tend to show colinear, often double, structure on the few kpc scale, similar to that seen in double sources on the 100 kpc scale. Identifications with quasars show much more distorted structure similar in kind to that seen in these four sources.

It is therefore plausible that the CSS quasars are driven by the same kind of central engine as the other types, but that the ejected material follows a much more tortuous path through the surrounding galaxy, either due to varying directions of the primary nozzle or due to a stronger interaction with the interstellar medium, or both. We are now studying these possibilities by means of multifrequency observations of these objects at radio wavelengths and optical, infrared, and X-ray wavelengths, and we will present a detailed interpretation of these observations in a further paper.

We wish to thank the US VLBI Network and the observers and technical staff of all the Network observatories involved in this work. In particular, we are extremely grateful to R. L. Mutel at North Liberty Radio Observatory, who generously built an entire receiving system for these observations. We also wish to thank R. A. Perley for the use of the unpublished 22.5 GHz VLA map of 3C 48. This work was supported in large part by the US National Science Foundation via grant AST 79-13249 to the Owens Valley Radio Observatory. We also gratefully acknowledge the support of a NATO travel grant. The National Radio Astronomy Observatory is operated by Associated Universities, Inc., under contract to the National Science Foundation. VLBI at the George R. Agassiz Station at Fort Davis, Texas is supported by the National Science Foundation.

REFERENCES

- Barthel, P. D., Pearson, T. J., and Readhead, A. C. S. 1988, *Ap. J. (Letters)*, **329**, L51.
- Clark, B. G. 1973, *Proc. IEEE*, **61**, 1242.
- Cohen, M. H. 1973, *Proc. IEEE*, **61**, 1192.
- Cornwell, T. J. 1986, in *Synthesis Imaging*, ed. R. A. Perley, F. R. Schwab, and A. H. Bridle (Green Bank: NRAO), p. 137.
- Cornwell, T. J., and Wilkinson, P. N. 1981, *M.N.R.A.S.*, **196**, 1067.
- . 1984, in *Indirect Imaging*, ed. J. A. Roberts (Cambridge: Cambridge University Press), p. 207.
- Davies, J. G., Anderson, B., and Morrison, I. 1980, *Nature*, **288**, 64.
- Fanti, C., Fanti, R., Parma, P., Nan, R., Schilizzi, R. T., van Bruegel, W. J. M., and Venturi, T. 1988 in *IAU Symposium 129, The Impact of VLBI on Astrophysics and Geophysics*, ed. M. J. Reid and J. M. Moran (Dordrecht: Reidel), p. 111.
- Fanti, C., Fanti, R., Parma, P., and Schilizzi, R. T. 1984, in *IAU Symposium 110, VLBI and Compact Radio Sources*, ed. R. Fanti, K. I. Kellermann, and G. Setti (Dordrecht: Reidel), p. 57.
- Fanti, C., Fanti, R., Parma, P., Schilizzi, R. T., and van Bruegel, W. J. M. 1985, *Astr. Ap.*, **143**, 292.
- Fanti, C., Fanti, R., Schilizzi, R. T., Spencer, R. E., and van Bruegel, W. J. M. 1986, *Astr. Ap.*, **170**, 10.
- Flatters, C. 1987, *Nature*, **326**, 6114.
- Ghigo, F., Rudnick, L., Wehinger, P., Wyckoff, S., Spinrad, H., and Johnston, K., 1986, in *IAU Symposium 119, Quasars*, ed. G. Swarup and V. K. Kapahi (Dordrecht: Reidel), p. 185.
- Hartas, J. S., Rees, W. G., Scott, P. F., and Duffett-Smith, P. J. 1983, *M.N.R.A.S.*, **205**, 625.
- Hewish, A. 1952, *Proc. Roy. Soc. London A*, **214**, 494.
- Jones, T. W., O'Dell, S. L., and Stein, W. 1974, *Ap. J.*, **188**, 353.
- Kapahi, V. K. 1981, *Astr. Ap. Suppl.*, **43**, 381.
- Kus, A. J., *et al.* 1990, in preparation.
- Kus, A. J., Wilkinson, P. N., and Booth, R. S. 1981, *M.N.R.A.S.*, **194**, 527.
- Moran, J. M. 1976, in *Methods of Experimental Physics* Vol. 12-Part C, ed. M. L. Meeks (New York: Academic), p. 228.
- Muxlow, T. W. B., Junor, W., Spencer, R. E., Simon, R., Benson, J. and Reid, M. J., 1988, in *IAU Symposium 129, The Impact of VLBI on Astrophysics and Geophysics*, ed. M. J. Reid and J. M. Moran (Dordrecht: Reidel), p. 131.
- Peacock, J. A., and Wall, J. V. 1982, *M.N.R.A.S.*, **198**, 843.
- Pearson, T. J., and Readhead, A. C. S. 1988, *Ap. J.*, **328**, 114.
- Readhead, A. C. S., and Hewish, A. 1974, *Mem. R.A.S.*, **78**, 1.
- Readhead, A. C. S., Kemp, M. C., and Hewish, A. 1978, *M.N.R.A.S.*, **185**, 207.
- Readhead, A. C. S., Napier, P. J., and Bignell, R. C. 1980, *Ap. J. (Letters)*, **237**, L55.
- Readhead, A. C. S., and Wilkinson, P. N. 1980, *Ap. J.*, **235**, 11.
- Schwab, F. R., and Cotton, W. D. 1983, *A.J.*, **88**, 688.
- Scott, M. A., and Readhead, A. C. S. 1977, *M.N.R.A.S.*, **180**, 539.
- Simon, R. S. 1983, Ph.D. thesis, California Institute of Technology.
- Simon, R. S., Dennison, B., Ananthakrishnan, S., and Fiedler, R. 1988, *Bull. AAS*, **19**, 1066.
- Simon, R. S., Readhead, A. C. S., Moffet, A. T., Wilkinson, P. N., Allen, B., and Burke, B. F. 1983a, *Nature*, **302**, 487.
- Simon, R. S., Readhead, A. C. S., Moffet, A. T., Wilkinson, P. N., and Anderson, B. 1980, *Ap. J.*, **236**, 707.
- Simon, R. S., Readhead, A. C. S., and Wilkinson, P. N. 1983b, in *IAU Symposium 110, VLBI and Compact Radio Sources*, ed. R. Fanti, K. I. Kellermann, and G. Setti (Dordrecht: Reidel), p. 109.
- Slee, O. B., and Wraith, P. K. 1967, *M.N.R.A.S.*, **214**, 971.
- van Brueghel, W., Miley, G., and Heckman, T., 1984, *A.J.*, **89**, 5.
- Wilkinson, P. N., *et al.* 1990, in preparation.
- Wilkinson, P. N., Booth, R. S., Cornwell, T. J., and Clark, R. R. 1984b, *Nature*, **308**, 619.
- Wilkinson, P. N., Conway, J. E., and Biretta, J. 1988, in *IAU Symposium 129, The Impact of VLBI on Astrophysics and Geophysics*, ed. M. J. Reid and J. M. Moran (Dordrecht: Reidel), p. 509.

Wilkinson, P. N., Cornwell, T. J., Kus, A. J., Readhead, A. C. S., and Pearson, T. J. 1984a, in *Physics of Energy Transport in Extragalactic Radio Sources*, ed. A. H. Bridle and J. A. Eilek (Green Bank: NRAO), p. 76.
 Wilkinson, P. N., Kus, A. J., Pearson, T. J., Readhead, A. C. S. and Cornwell, T. J., 1986, in *IAU Symposium 119, Quasars*, ed. G. Swarup and V. K. Kapahi (Dordrecht: Reidel), p. 165.

Wilkinson, P. N., Readhead, A. C. S., Purcell, G. H., and Anderson, B. 1977, *Nature*, **269**, 764.

Wilkinson, P. N., Spencer, R. E., Readhead, A. C. S., Pearson, T. J., and Simon, R. S., 1984c, in *IAU Symposium 110, VLBI and Compact Radio Sources*, ed. R. Fanti, K. I. Kellermann, and G. Setti (Dordrecht: Reidel), p. 25.

B. ALLEN: TRW, Redondo Beach, CA

R. BOOTH: Chalmers Technical University, Onsala Space Observatory, Onsala, Sweden

B. F. BURKE: Department of Physics, Massachusetts Institute of Technology, Cambridge, MA 01002

A. T. MOFFET: Deceased

A. C. S. READHEAD: California Institute of Technology, Pasadena, CA 91125

R. S. SIMON: E. O. Hulburt Center for Space Research, Naval Research Laboratory, Washington, DC 20375

P. N. WILKINSON: Nuffield Radio Astronomy Laboratories, Jodrell Bank, Macclesfield, Cheshire, SK11 9DL England, UK